BIOCHEMISTRY
including biophysical chemistry & molecular biology

Article

pubs.acs.org/biochemistry

α-Helical Domains Affecting the Oligomerization of Vipp1 and Its Interaction with Hsp70/DnaK in *Chlamydomonas*

Fei Gao,*[,†] Wenyan Wang,[‡] Wenjuan Zhang,[†] and Cuimin Liu*[,†]

[†]State Key Laboratory of Plant Cell and Chromosome Engineering, Institute of Genetics and Developmental Biology, Chinese Academy of Sciences, Beijing 100101, China

[‡]School of Pharmacy, Yantai University, No. 30 Qingquan Road, Laishan District, Yantai City, Shandong 264005, China

Supporting Information

ABSTRACT: Vesicle-inducing protein in plastids 1 (Vipp1) forms >1 MDa ordered homo-oligomeric complexes in chloroplasts and is involved in the biogenesis of photosynthetic machinery. The Hsp70 chaperone system has been shown to interact with Vipp1, influencing its higher-order structure. In this study, a series of deletion mutants in *Chlamydomonas reinhardii* Vipp1 (CrVipp1) is used to investigate the role of the α-helical domains (H1−H7) in mediating its structure and interaction with DnaK, an Hsp70 orthologue. Results from these analyses demonstrate that α-helical domains H1−H6 of CrVipp1 are required for its efficient accumulation in protease-resistant large complexes, termed super-oligomers. Deletions of these α-helical domains, either individually or in combination, cause CrVipp1 to assemble into a heterogeneous mixture of smaller, protease-sensitive oligomers. Furthermore, domains H2 and H3 are required to form a stable structural core in mutant oligomers, whereas domains H1 and H4−H6 likely function downstream in assembly of the superoligomer. DnaK binds only weakly to any form of CrVipp1 that efficiently assembles into superoligomers. In contrast, the interaction with DnaK is much more robust with certain misfolded CrVipp1 oligomers in a process mediated by their H4 and H7 domains. DnaK also interacts with full-length CrVipp1 at an early stage of CrVipp1 biosynthesis, perhaps during initial steps in the oligomerization pathway. Taken together, these data suggest that not only α-helical domains but also the oligomeric states of CrVipp1 influence its interaction with DnaK. It is therefore plausible that the Hsp70/DnaK system may be involved in the assembly of Vipp1 superoligomers.

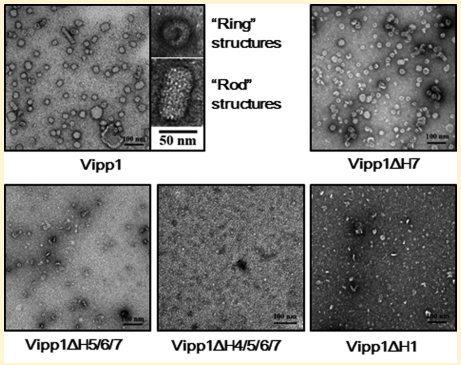

Thylakoids are important structures of cyanobacteria and chloroplasts, in which the major complexes of oxygenic photosynthesis are embedded. In thylakoids, although protein complexes that take part in oxygenic photosynthesis are well understood, substantially less is known about thylakoid membrane biogenesis. Vesicle-inducing protein in plastids 1 (Vipp1) was first described by Keegstra and co-workers in a pea chloroplast.[1] They found that this 30 kDa protein is associated with both inner and outer membranes of thylakoids. Vipp1 mutants in *Arabidopsis thaliana* in which the level of expression of AtVipp1 was greatly reduced were subsequently identified,[2] and these mutant plants lost the ability to perform oxygenic photosynthesis because of the disruption of the thylakoid membrane system. Vipp1 mutants were found to be deficient in chloroplast vesicle formation, and with this phenotype in mind, the authors designated the protein as Vipp1. A similar phenotype was also described for Vipp1 deletion mutants in *Synechocystis*.[3] It was suggested that Vipp1 may be required for transporting galactolipids from the inner envelope of chloroplasts to thylakoids.[4−6] Additionally, Vipp1 is involved in the assembly of photosynthesis complexes in cyanobacteria and chloroplasts,[7−9] and a role of Vipp1 in the cpTat protein transport system was also reported.[10] It has been suggested that Vipp1 may be involved in the transport of protein from the cytoplasm into the chloroplast and play important roles in assembly of the photosynthesis apparatus.

Vipp1 is highly homologous with the *Escherichia coli* protein phage shock protein A (PspA). PspA was first characterized in the process of filamentous phage infection of *E. coli* cells.[11] In *E. coli*, PspA is a member of the bacterial stress response system that responds to invasion by filamentous phages, inhibition of lipid biosynthesis, blockage of protein export machinery, and different stress factors such as heat, organic solvents, and hyperosmotic conditions.[12] It is clear that PspA helps to sustain the proton motive force and maintain membranes under stress conditions.[13−15] It was recently elucidated that Vipp1 functions like PspA in protecting chloroplast membranes in *Arabidopsis*.[16] Furthermore, Vipp1 could replace PspA function to some extent in *E. coli*,[17] but functional diversification of Vipp1 and PspA is indeed evident because PspA does not compensate for *vipp1* deletion in *Synechocystis*.[3]

Vipp1 is highly similar to PspA in amino acid sequence, and they may share a common ancestor according to phylogenetic analysis.[12] According to secondary structural analysis, predom-

Received: January 19, 2015
Revised: July 8, 2015
Published: July 30, 2015

DOI: 10.1021/acs.biochem.5b00050
Biochemistry 2015, 54, 4877−4889

inant α-helical structures are present in both Vipp1 and PspA. Only a few amino acids, which are predicted to be random-coil domains, interrupt the helical domains. Notably, Vipp1 contains an additional C-terminal domain containing one α-helical domain and an adjacent random coil with amino acids of variable length in different species.[18−20] This distinct C-terminal domain may have allowed Vipp1 to acquire specialized functions in higher plants that distinguish it from PspA. The tertiary structures of Vipp1 and PspA also share some similar characteristics. Both are able to form huge homologous ring-shaped complexes with molecular masses of >1 MDa.[18,19,21,22] When PspA protein was subdivided into four helical domains termed H1−H4 and oligomerization of the resulting truncated PspA proteins was analyzed in *E. coli*, it was found that the H2 or H3 domain alone can form hexamers of PspA, and the H4 domain helps PspA form a 36mer ring structure.[12]

In contrast to that of PspA, the Vipp1 structure is more complex in nature. In addition to forming ring-shaped oligomers, Vipp1 also forms barrel-like or rod-like structures.[18,19,22] Recent work has shown that the N-terminal α-helix of Vipp1 containing the first 21 amino acids was essential for both the formation of very large homo-oligomers of Vipp1, termed superoligomers, and the interaction of Vipp1 with the inner membrane of the chloroplast in *Arabidopsis*.[23] Furthermore, the dynamic structure of Vipp1 may be controlled by the chaperone systems. Indeed, Vipp1 interacts with Hsp70/DnaK, which was able to catalyze the assembly of Vipp1 oligomers with the help of CDJ2 and CGE1.[22,24]

In this work, a series of deletion mutants of CrVipp1 were designed to identify α-helical domains that impact the oligomerization of CrVipp1 and its interaction with Hsp70/DnaK. Here, we demonstrate that the H1−H6 α-helical domains of CrVipp1 are important for its accumulation in large superoligomeric complexes. Deletion of H1−H6, either alone or in combination, caused CrVipp1 to assemble into a heterogeneous mixture of smaller oligomers, which were more vulnerable than full-length proteins in proteinase digestion experiments. Our data indicate that H1−H6 have differentiated functionally. Domains H2 and H3 formed a protease-resistant core in mutant oligomers, pointing toward their structural importance, whereas domains H1 and H4−H6 likely function downstream in the assembly of compact superoligomers. Moreover, we demonstrate that DnaK binds weakly to any form of CrVipp1 that has efficiently achieved its superoligomeric conformation, whether it be steady state levels of full-length CrVipp1 or the H7 mutant that oligomerizes normally. The interaction with DnaK was dramatically enhanced with certain misfolded mutants of CrVipp1 that cannot efficiently form superoligomers and/or are sensitive to protease digestion. This robust interaction with DnaK was mediated by the H4 and H7 domains exposed in misfolded oligomers of CrVipp1. DnaK was also found to bind to full-length CrVipp1 shortly after its synthesis, likely during early steps in the oligomization pathway. Taken together, these data are consistent with the notion that not only α-helical domains but also the oligomerization status of CrVipp1 affects its interaction with DnaK. It is well-known that there are several forms of CrVipp1, monomer and/or dimer and large superoligomers, that accumulate *in vivo*,[22,25] and it follows that Hsp70/DnaK or probably other unknown factors specifically interact with certain conformational states of CrVipp1 via exposed α-helical domains to promote assembly into the native states.

MATERIALS AND METHODS

Cloning, Expression, and Purification of Recombinant CrVipp1 and Truncated CrVipp1 Proteins. The coding region of CrVipp1 (without a signal peptide) was amplified by polymerase chain reaction (PCR) from cDNA clone AV632440 ordered from the Kasuza Institute (for primer pairs, see Table S1 of the Supporting Information).[26] A 753 bp PCR product was digested and ligated into expression vector pET11a (Novagen). Plasmid pET11a-CrVipp1 was transformed into *E. coli* BL21(DE3) and induced by 0.5 mM isopropyl β-D-galactopyranoside (IPTG) for 3 h at 37 °C. Cells were harvested and suspended in lysis buffer [20 mM Tris-HCl (pH 8.0), 20 mM NaCl, 1 mM EDTA, and 1 mM PMSF]. The suspended cells were broken by ultrasonication (Sonicator S-4000, Misonix), and the soluble sample from centrifugation was subjected to a Source 30Q column (GE Healthcare). After detection by SDS−PAGE, fractions containing CrVipp1 were dialyzed against the dialysis buffer [20 mM Tris-HCl (pH 8.0) and 20 mM NaCl] overnight and then applied to a Mono Q column (GE Healthcare). After being detected by SDS−PAGE, fractions containing CrVipp1 were concentrated and subjected to a Hiload 16/60 Superdex 200 column (GE Healthcare) in storage buffer [20 mM Tris-HCl (pH 8.0), 20 mM NaCl, and 1 mM EDTA]. CrVipp1 protein was then concentrated, frozen in liquid nitrogen, and stored at −80 °C. The protein concentration was determined by spectrophotometry (Astra-Net).

Truncated CrVipp1 genes were amplified by use of different primer pairs (Table S1 of the Supporting Information) from cDNA clone AV632440. PCR products were digested and ligated into the pET22b vector (Novagen). Constructed expression plasmids were transformed into *E. coli* BL21(DE3). Transformed cells were induced by 0.5 mM isopropyl β-D-galactopyranoside (IPTG) for 3 h at 37 °C. Cells were harvested and suspended in lysis buffer [20 mM Tris-HCl (pH 8.0), 20 mM NaCl, 1 mM EDTA, and 1 mM PMSF]. The suspended cells were broken by ultrasonication (Sonicator S-4000, Misonix). The truncated CrVipp1 proteins were purified with a Ni-NTA column according to the standard procedure (Novagen). Purified truncated CrVipp1 proteins were dialyzed extensively at 4 °C against buffer [20 mM Tris-HCl (pH 8.0) and 50 mM NaCl]. CrVipp1 protein was then concentrated, frozen in liquid nitrogen, and stored at −80 °C. The protein concentration was determined by spectrophotometry (Astra-Net), and all truncated proteins were centrifuged at 16000*g* for 20 min at 4 °C to remove the unspecific particles and aggregates before all experiments were performed.

Circular Dichroism Spectroscopy. The secondary structure of the truncated CrVipp1 variants was analyzed with a Chirascan-plus CD spectrometer (Applied Photophysics Ltd.) using 1 mm cuvettes. The truncated CrVipp1 proteins were diluted to 0.1 μg/μL in PBS buffer (8 g/L NaCl, 0.2 g/L KCl, 1.46 g/L Na_2HPO_4, and 0.2 g/L KH_2PO_4) and analyzed. Wavelength scans were recorded at 20 °C over a wavelength range of 195−260 nm. The bandwidth was set to 1 nm and the scanning speed to 1 nm/s. For each protein spectrum, three scans were averaged and the data were deconvoluted by using CDNN software (http://bioinformatik.biochemtech.uni-halle.de/cdnn).

Proteinase Digestion Assay. The proteinase digestion assay was conducted in the buffer [20 mM Tris-HCl (pH 8.0) and 50 mM NaCl] containing 3 μg of protein, followed by

DOI: 10.1021/acs.biochem.5b00050
Biochemistry 2015, 54, 4877−4889

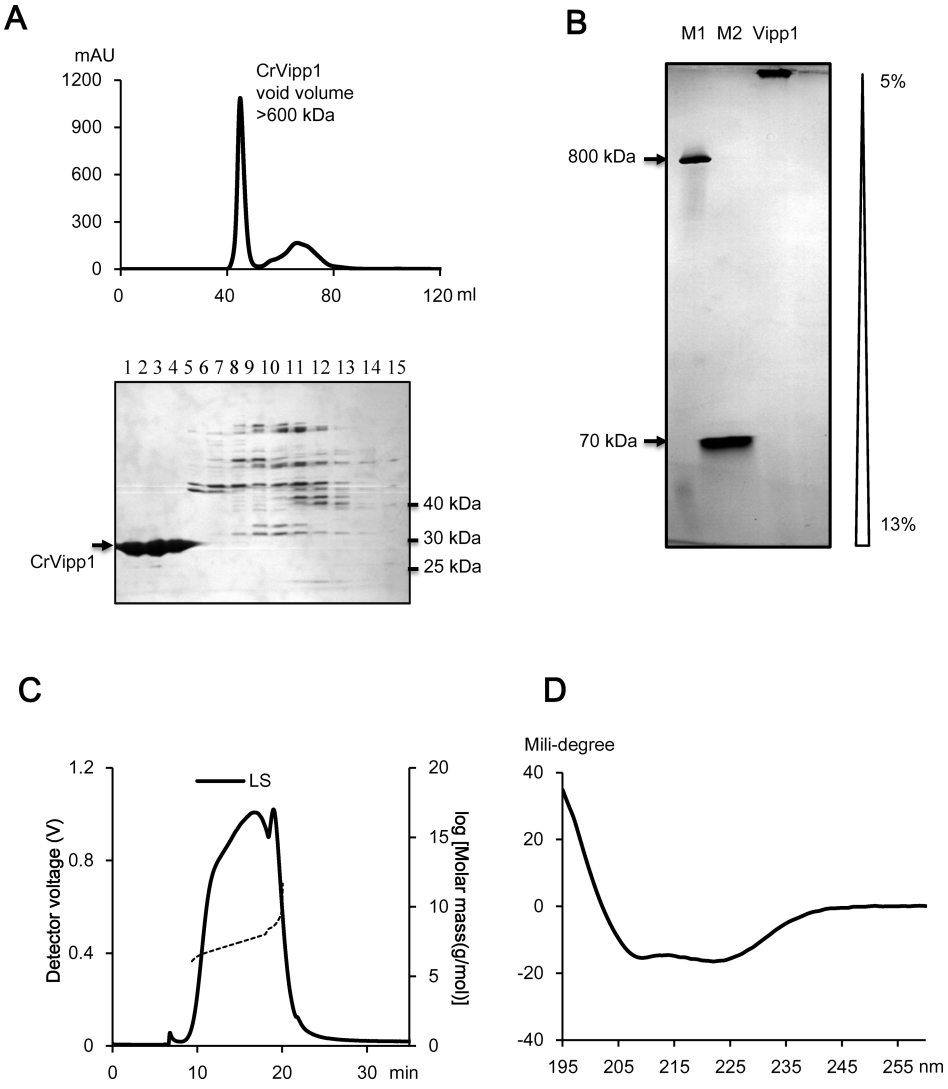

Figure 1. Structural analysis and purification of mature CrVipp1 *in vitro*. (A) The protein pool was separated on a gel filtration column (Hiload 16/60 Superdex 200, GE), and the eluted fractions of 44−76 mL were separated by 12% SDS−PAGE. (B) Analysis of recombinant CrVipp1 with a colorless native gel. GroEL in lane M1 is ∼800 kDa, while GroES in lane M2 is ∼70 kDa. (C) Profiles of the status of the CrVipp1 superoligomeric complex in AFFFF analysis. LS means the signal strength of the laser detector of AFFFF shown on the left *y*-axis, and molar mass means the molecular weight of the full-length CrVipp1 superoligomeric complex shown on the right *y*-axis. Experiment conditions: elution flow of 0.8 mL/min and cross-flow of 0.5 to 0 mL/min. (D) Circular dichroism spectrum of purified CrVipp1 protein. The *y*-axis values are the raw data from the Chirascan-plus CD spectrometer.

addition of the indicated amount of subtilisin proteinase (PS, Sigma). The reaction mixture was incubated for 60 min at 4 °C and the reaction stopped with 1 mM phenylmethanesulfonyl fluoride (PMSF). The fractions from proteinase reactions were resolved by SDS−PAGE with Coomassie staining.

Native PAGE, SDS−PAGE, and Western Blotting. The Native PAGE (colorless native gel) procedure was conducted according to a published protocol;[24] 15 μg of purified protein was loaded onto a 5 to 13% gradient colorless native gel. The SDS−PAGE procedure was performed as described previously;[27] 1 μg of purified protein was loaded onto a 15% SDS−PAGE gel. Proteins in gels were stained with Coomassie or transferred to ECL membranes (Hybond-ECL, Amersham Biosciences) by a semidry transfer system. Blocking was performed in PBS buffer containing 5% nonfat dry milk (BD). Proteins transferred to membranes were detected by serum anti-CrVipp1 (produced in rabbit at our institute facilities), anti-DnaK (produced in rabbit at our institute facilities), or anti-His tag (Abmart). The chemiluminescence from HRP-labeled goat anti-rabbit IgG (Sigma) was detected with ECL solutions [100 mM Tris-HCl (pH 8.5), 2.5 mM Luminol (Sigma), 0.4 mM *p*-coumaric acid (Sigma), and 0.000183% H_2O_2] and imaged by an imageQuant LAS 4000 apparatus (GE Healthcare).

Pull-Down Assay. For pull-down assays, pET22b-truncated CrVipp1 and pG-KJE8 (TaKaRa) plasmids were cotransformed into *E. coli* BL21(DE3), and transformed cells were grown at 37 °C until the OD_{600} reached 0.6. After induction of the DnaK system for 2 h via addition of L-arabinose (0.2%), the cells were collected and resuspended in medium containing 1 mM isopropyl β-D-galactopyranoside (IPTG) to induce expression of the CrVipp1 protein variants for 3 h at 37 °C. Alternatively, the proteins were induced for various time as indicated by adding 0.2% L-arabinose and 1 mM IPTG (Figure 6). The cells were centrifuged and suspended in 1 mL of pull-down lysis buffer [50 mM NaCl, 10 mM imidazole, 20 mM Tris-HCl (pH

DOI: 10.1021/acs.biochem.5b00050
Biochemistry 2015, 54, 4877−4889

8.0), and 1 mM PMSF]. After cell membrane disruption by ultrasonification (Sonicator S-4000, Misonix), cell material was centrifuged at 13400*g* and 4 °C for 20 min, and the supernatant was incubated with Ni-NTA beads for 15 min at 4 °C while being gently shaken. The beads were centrifuged and washed four times with 1 mL of pull-down wash buffer [50 mM NaCl, 25 mM imidazole, and 20 mM Tris-HCl (pH 8.0)]. The protein was eluted from beads with 120 μL of elute buffer [50 mM NaCl, 500 mM imidazole, and 20 mM Tris-HCl (pH 8.0)]. All operations of pull-down experiments were conducted on ice. A volume of 10 μL of eluate was separated by 15% SDS−PAGE and detected by Coomassie staining or Western blotting.

The relative amount of pulled down DnaK to CrVipp1 was determined by measuring the signal intensity on the blotting membrane using ImageJ software, and the quantification revealed the ratio of signal intensity of pulled down DnaK to that of CrVipp1.

Asymmetric Flow Field Flow Fractionation−Multi-angle Light Scattering (AFFFF−MALS). For detecting the status of purified truncated CrVipp1 proteins, all truncated proteins were centrifuged at 16000*g* and 4 °C for 20 min to remove the unspecific particles and aggregates, and 40 μg of protein was analyzed by an asymmetric flow field flow fractionation (AFFFF) system (Eclipse AF4, Wyatt Technology, Santa Barbara, CA) using a 350 μm spacer and a 10 kDa RC membrane (Wyatt Technology) with an elution flow of 0.8 mL/min and a different cross-flow in running buffer [20 mM Tris-HCl (pH 8.0) and 150 mM NaCl]. The AF4 device was connected with a multiangle light scattering system (DAWN HELEOS II, Wyatt Technology, wavelength of 658 nm), a Nanostar (Wyatt Technology, wavelength of 658 nm), a variable-wavelength detector (absorbance at 280 nm, Agilent 1100 series), and a differential refractive index detector (dRI) (Optilab rEX, Wyatt Technology, wavelength of 660 nm). The molar mass was calculated using ASTRA 6 (Wyatt Technology).

Gel Filtration Assay. All purified CrVipp1 proteins were centrifuged at 16000*g* and 4 °C for 20 min to remove the unspecific particles and aggregates and subjected to a Superose 6 PC 3.2/30 column (bed volume of 2.4 mL) (GE Healthcare) with running buffer [20 mM Tris-HCl (pH 8.0) and 50 mM NaCl] at a flow rate of 60 μL/min. The fractions were collected and loaded on the SDS−PAGE gel.

Matrix-Assisted Laser Desorption Ionization Time-of-Flight (MALDI-TOF) Mass Spectra. Full-length CrVipp1 and proteinase-digested CrVipp1 were desalted with ZipTip C18 (Millipore) before being applied to the MALDI-TOF mass spectrometer. The samples were analyzed using an Axima-CFRTM plus MALDI-TOF mass spectrometer (Kratos/Shimadzu Biotech, Manchester, U.K.) equipped with a pulsed nitrogen laser operated at 337 nm. Positive ion MALDI mass spectra were acquired in linear mode with a mass range (m/z) of 15000−45000. Prior to the analysis of samples, the Axima-CFR TM plus instrument was externally calibrated with apomyoglobin ($[M + H]^+$ average of 16952.5) and aldolase ($[M + H]^+$ average of 39212.8).

Transmission Electron Microscopy (TEM). Four microliters at a concentration of 0.1 g/L for any given sample, the purified CrVipp1 complex or its truncated variants, was adsorbed for 1 min onto carbon-coated grids previously hydrophilized by glow discharge. Excess protein sample was then removed from the carbon support by blotting and the grid washed rapidly with water prior to being stained with 1% uranyl acetate for ∼1 min and then air-dried. Images were recorded using an OSIS MEGAVIEW G2 (1K × 1K) CCD digital camera system (Olympus, Tokyo, Japan) at an accelerating voltage of 120 keV on an FEI Spirit transmission electron microscope (FEI, Eindhoven, The Netherlands).

RESULTS

Structural Analysis of *Chlamydomonas* Vipp1 *in Vitro*. CrVipp1 is a chloroplast protein encoded in the nucleus whose 37 N-terminal amino acids of precursor protein are cleaved upon translocation into the chloroplast. To investigate the oligomeric state of the mature protein, Vipp1 cDNA from *Chlamydomonas* was ordered from the Kazusa Institute and an *E. coli* expression plasmid encoding mature protein was constructed (CrVipp1). CrVipp1 protein was induced and prepurified by chromatography with Source 30Q and Mono Q columns without any detergent. CrVipp1 was further purified with a Superdex 200 column and eluted in the void volume with a molecular mass of >600 kDa (Figure 1A, bands 1−3, 43−48 mL), which is in accordance with the size of Vipp1 previously reported in *Arabidopsis* and *Chlamydomonas*.[18,22,23] Minor A_{280} absorbance corresponding to a molecular mass of ∼60−100 kDa was due to other unknown proteins (Figure 1A, bands 4−12, 57−74 mL). AFFFF, native gel methods, and transmission electron microscopy were used to further study the oligomeric status of CrVipp1. In the native gel, one single band that barely entered the separating gel was detected, indicating that CrVipp1 formed large complexes with masses far greater than 800 kDa (Figure 1B) that are hereafter termed superoligomers. AFFFF analysis showed that the molar mass of CrVipp1 is greater than 1 MDa (Figure 1C), indicating that CrVipp1 superoligomers are composed of 36 subunits, similar to its homologue PspA. Results from an electron microscopy assay (Figure 4D) showed that CrVipp1 formed ring structures with different diameters that are potentially incorporated into rod-like structures, consistent with previous reports.[18,19,21] To check if the superoligomers might result from protein aggregation, the protein was centrifuged for 20 min at 200000*g* and the supernatant was subjected to AFFFF again with the same result (data not shown). CrVipp1 was also subjected to circular dichroism spectroscopy and deconvoluted with CDNN software.[28,29] It was shown that ∼75% of CrVipp1 was helical and 25% of CrVipp1 was random coil or other secondary structure (Figure 1D and Table 1). The ratio of the molar ellipticity at 208 nm to that at 222 nm was <1, indicating CrVipp1 forms highly ordered coiled-coil structures (Table 1).[30]

Vipp1 protein in photosynthetic organisms is largely homologous with PspA from *E. coli* and *Synechocystis* sp. except for its C-terminal extension of ∼30 amino acids. Asseva et al. found that the C-terminal extension extrudes from a highly ordered ring structure of Vipp1 in *Arabidopsis*.[18] To assess the flexibility of the C-terminus, CrVipp1 was digested with the unspecific proteinase subtilisin. After cleavage, one fragment migrating at ∼24 kDa was relatively stable (Figure 2A, CrVipp1*). MALDI-TOF mass spectrometry was used to determine that the mass of this stable fragment of CrVipp1 was actually 24524 g/mol (Figure 2B). This estimation is consistent with removal of the 28 C-terminal amino acids (224−251). Indeed, the 35 C-terminal amino acids (216−251) were not detected by Q-TOF mass spectrometry (data not shown), suggesting that the C-terminus is exposed from the CrVipp1

DOI: 10.1021/acs.biochem.5b00050
Biochemistry 2015, 54, 4877−4889

Table 1. Content of Helical Structure in Truncated CrVipp1 Proteins As Determined by Circular Dichroism Spectroscopy

	CK	Vipp1	Vipp1ΔH7	Vipp1ΔH5/6/7	Vipp1ΔH4/5/6/7	Vipp1ΔH4/5/6	Vipp1ΔH1	Vipp1ΔH1/2	Vipp1ΔH1/2/7	Vipp1ΔH3	Vipp1ΔH3/7
helix	0.74	0.71	0.73	0.81	0.81	0.82	0.85	0.89	0.89	0.86	0.89
others	0.26	0.29	0.27	0.19	0.19	0.17	0.15	0.11	0.11	0.14	0.11
208 nm/222 nm	0.91	0.85	0.90	0.97	0.98	1.01	1.08	1.46	1.58	1.12	1.29

superoligomeric structures and therefore sensitive to proteinase treatment, consistent with what was observed with *Arabidopsis* AtVipp1.[18] The secondary structure of CrVipp1 was then predicted with Jpred3.[19] As shown in Figure 2C (top "Vipp1" schematic), seven α-helical structures (H1−H7) interrupted with random coils were predicted. The 28 flexible C-terminal amino acids corresponded to H7, with amino acids 50−78 of H2 and the entire region of H3 predicted to form coiled-coil structures.

Influence of Helical Domains on the Stability of CrVipp1 in the Presence of Proteinase. According to the predicted secondary structure, a series of truncated CrVipp1 proteins containing different α-helical domains were generated (Figure 2C). The H5 and H6 regions contained only very short α-helical domains that corresponded to one single α-helix in PspA.[20] Therefore, regions H5 and H6 were considered practically as a single α-helix and were not deleted separately. To facilitate purification, all truncated CrVipp1 proteins (including full-length CrVipp1) were constructed with a six-His tag at the C-terminus of the protein and all proteins were purified by Ni^{2+} affinity chromatography without any detergent. CrVipp1 and CrVipp1-His showed no difference in native gel, AFFFF, or transmission electron microscopy analysis (data not shown). Analysis by SDS−PAGE after centrifugation and transmission electron microscopy indicated that all truncated proteins accumulated as soluble and stable proteins with the expected molecular weight (Figures 3A and 4D, some data not shown). Circular dichroism spectroscopy was then used to assess proper folding and the overall α-helical structure of the proteins. As shown in Figure 3B and Table 1, all truncated proteins were helical in structure as expected, and the content of helical structures, ranging from 70 to 90%, was reasonable considering the deletions of helical domains of CrVipp1. Notably, the ratios of the molar ellipticity at 208 nm to that at 222 nm are <1 in Vipp1, Vipp1ΔH7, Vipp1ΔH5/6/7, and Vipp1ΔH4/5/6/7, which indicated that these proteins may form coiled-coil structures (Table 1).

To investigate the stability of truncated CrVipp1 proteins, purified proteins were treated with subtilisin proteinase. Vipp1ΔH7 was very stable, resisting proteinase digestion in the presence of up to 5 μg/mL subtilisin (Figure 3C). These results are consistent with the digestion of full-length CrVipp1, in which a fragment presumably lacking the H7 domain was largely resistant to degradation at similar protease concentrations (Figure 2A, lower band). Deletion of N-terminal H1 resulted in increased sensitivity to proteinase (Figure 3D), while deletion of coiled-coil domains (H2 and H3) also increased the sensitivity to proteinase (Figure 3E,F). Deletion of H5−H7 or H4−H7 also caused further increased sensitivity to proteinase (Figure 3G,H). Taken together, these data indicate that all α-helical regions, except for H7, are required for formation of the compact, protease-resistant, structure of CrVipp1. A small fragment at ∼17 kDa was detected under Vipp1ΔH1, Vipp1ΔH5/6/7, and Vipp1ΔH4/5/6/7 conditions (Figure 3D,G,H), while this 17 kDa small fragment disappeared in the cases of Vipp1ΔH1/2 and Vipp1ΔH3 (Figure 3E,F). On the basis of this result, it is likely that this protease-resistant 17 kDa fragment might be a part of the coiled-coil domains (H2 and H3) that might form another compact structure.

Effect of α-Helical Domains on the Formation of a CrVipp1 Superoligomer. To check the effect of α-helical domains on the oligomeric state of the CrVipp1 protein, equal amounts of truncated protein were analyzed by native gel and

DOI: 10.1021/acs.biochem.5b00050
Biochemistry 2015, 54, 4877−4889

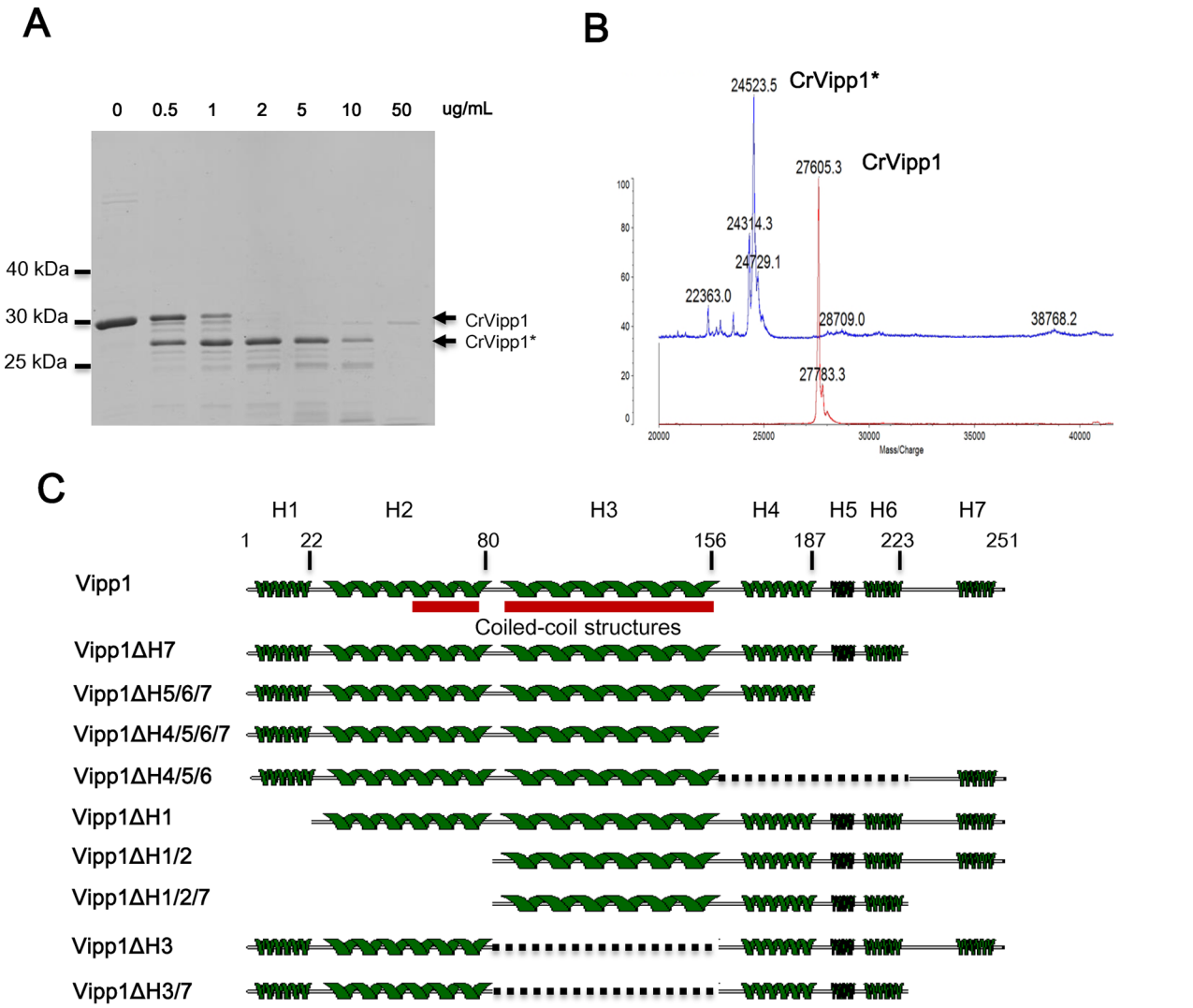

Figure 2. C-Terminal helical domain of CrVipp1 that is excluded from the tertiary structure. (A) Treatment of CrVipp1 with subtilisin proteinase at different concentrations (0, 0.5, 1, 2, 5, 10, and 50 μg/mL). "CrVipp1" indicates full-length CrVipp1 (~28 kDa), and "CrVipp1*" (~24 kDa) denotes the major product from the digestion. (B) Analysis by mass spectrometry. The molecular weight of purified CrVipp1 was 27606 Da, and that of the digested product was 24534 Da. (C) Prediction of CrVipp1 secondary structure by Jpred3. CrVipp1 has seven α-helices: H1, amino acids 1−22; H2, amino acids 25−80 containing coiled-coil structures; H3, amino acids 84−156 containing coiled-coil structures; H4, amino acids 164−187; H5, amino acids 193−201; H6, amino acids 204−217; H7, amino acids 235−251. The following CrVipp1 constructs were used in this study: Vipp1, full-length CrVipp1; Vipp1ΔH7, CrVipp1 with a deletion of amino acids 224−251; Vipp1ΔH5/6/7, CrVipp1 with a deletion of amino acids 188−251a; Vipp1ΔH4/5/6/7, CrVipp1 with a deletion of amino acids 157−251; Vipp1ΔH4/5/6, CrVipp1 with a deletion of amino acids 157−223; Vipp1ΔH1, CrVipp1 with a deletion of amino acids 1−22; Vipp1ΔH1/2, CrVipp1 with a deletion of amino acids 1−80; Vipp1ΔH1/2/7, CrVipp1 with deletions of amino acids 1−80 and 224−251; Vipp1ΔH3, CrVipp1 with a deletion of amino acids 81−156; Vipp1ΔH3/7, CrVipp1 with deletions of amino acids 81−156 and 224−251.

size exclusion chromatography followed by SDS−PAGE (Figure 4A,B). Vipp1ΔH7 behaved like full-length Vipp1, accumulating efficiently as superoligomeric complexes as shown by native PAGE and eluting earlier than GroEL from a Superose 6 PC 3.2/30 column with a separation range of 5 kDa to 5 MDa. These results suggested that the H7 domain is not essential for the formation of CrVipp1 superoligomeric complexes, which is also in good agreement with the results of previous proteinase digestion experiments (Figures 2A and 3C). C-Terminal deletions of three or four helical domains (Vipp1ΔH5/6/7 and Vipp1ΔH4/5/6/7) revealed a substantial change in the status of CrVipp1 oligomers (Figure 4A,B). Vipp1ΔH5/6/7 was able to form >1 MDa superoligomers; however, the tendency to form these oligomers decreased dramatically, and smaller oligomers, including dimers, etc., were also present. Superoligomeric complexes were nearly absent under the Vipp1ΔH4/5/6/7 condition, and a population of smaller oligomers formed. On the other hand, truncated protein Vipp1ΔH4/5/6 accumulated in oligomers slightly larger than those of Vipp1ΔH4/5/6/7. Among the N-terminal deletions, deletion of H1 and H2 (Vipp1ΔH1/2), but not deletion of H1 alone (Vipp1ΔH1), largely abolished superoligomeric complexes, indicating H2 plays an essential role in the formation of superoligomers (Figure 4A,B). Vipp1ΔH3 and Vipp1ΔH3/7 formed low levels of superoligomeric complexes as well as smaller oligomeric complexes; however, Vipp1ΔH3, but not Vipp1ΔH3/7, preferentially accumulated in larger oligomers (Figure 4A,B). In addition, the AFFFF assay was also used to test the oligomeric state of truncated CrVipp1. As shown in Figure 4C, Vipp1ΔH7, like full-length Vipp1, formed

DOI: 10.1021/acs.biochem.5b00050
Biochemistry 2015, 54, 4877−4889

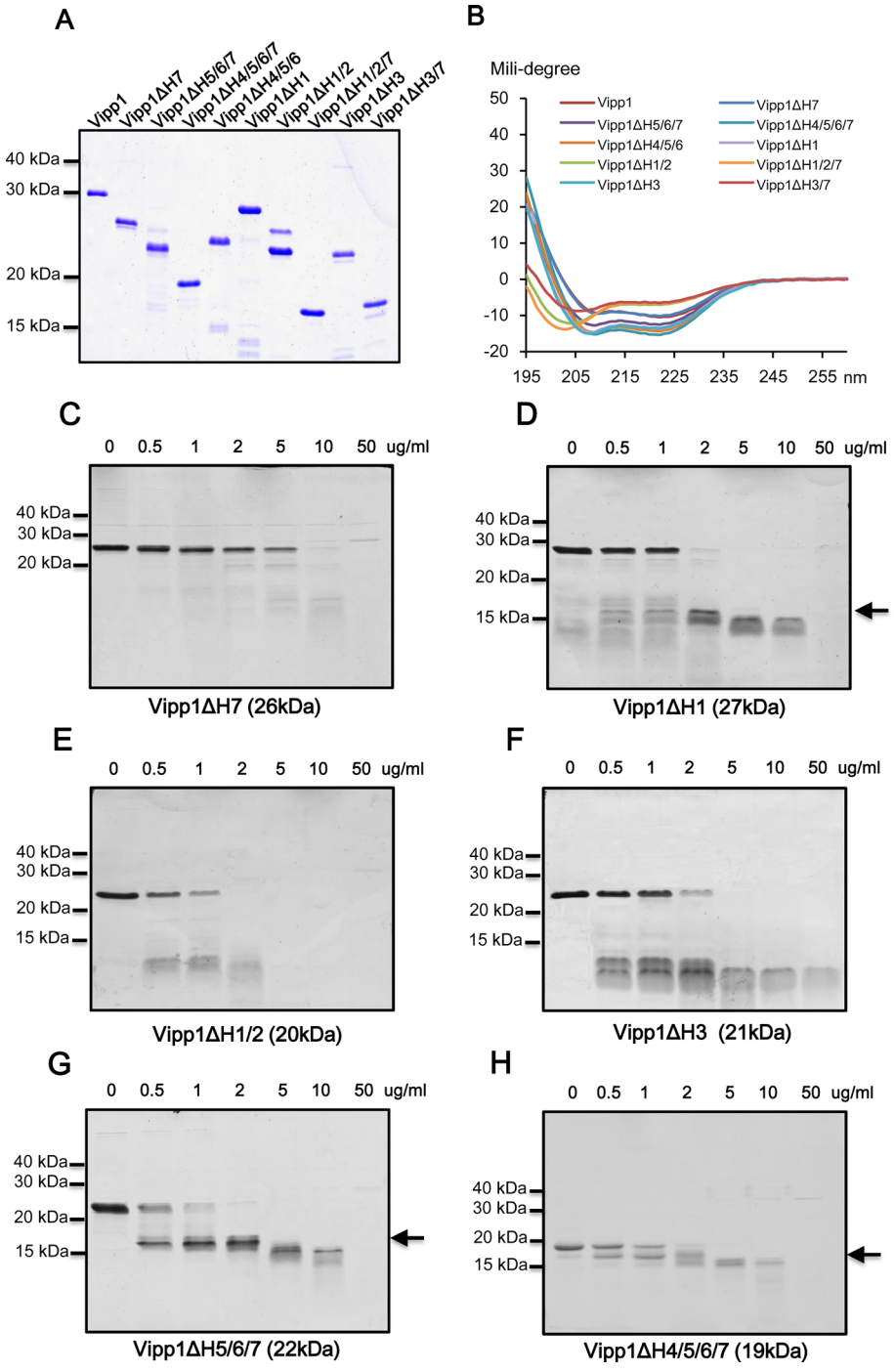

Figure 3. Preparation of truncated CrVipp1 mutants. (A) Purified truncated protein resolved by SDS−PAGE. The truncated protein was purified with a His tag affinity chromatography column, and 1 μg of protein was separated by 15% SDS−PAGE with Coomassie staining. (B) Circular dichroism spectroscopy curves of purified truncated CrVipp1 proteins. The *y*-axis values are the raw data from the Chirascan-plus CD spectrometer. Different colored lines indicate different truncated CrVipp1 proteins. (C−H) Truncated CrVippp1 proteins were digested by subtilisin proteinase at different concentrations (0, 0.5, 1, 2, 5, 10, and 50 μg/mL subtilisin, respectively). The arrows represent the small fragment at ∼17 kDa.

>1 MDa superoligomers; Vipp1ΔH4/5/6/7 did not form high-molecular weight oligomers, and other truncated proteins all demonstrated similar profiles of monomers to high-molecular weight oligomers present (Figure 4C and data not shown). To confirm the outcomes from native gels, gel filtration, and AFFFF visually, single-particle work was conducted. TEM on negatively stained samples showed that full-length Vipp1 proteins formed ring-like structures with various diameters, with some rings double or triple the diameter of others (Figure 4D). The rod-like structures were also observed as previously reported.[18,19,22] Large ring-like structures of the Vipp1ΔH7 mutant protein were also observed, but no rod-like structures were detected (Figure 4D). Fewer and smaller ring-like structures of truncated proteins (Vipp1ΔH4/5/6/7, Vipp1ΔH5/6/7, and Vipp1ΔH1) were visualized, suggesting that the ability to form large superoligomeric complexes was abolished in these mutants.

DOI: 10.1021/acs.biochem.5b00050
Biochemistry 2015, 54, 4877−4889

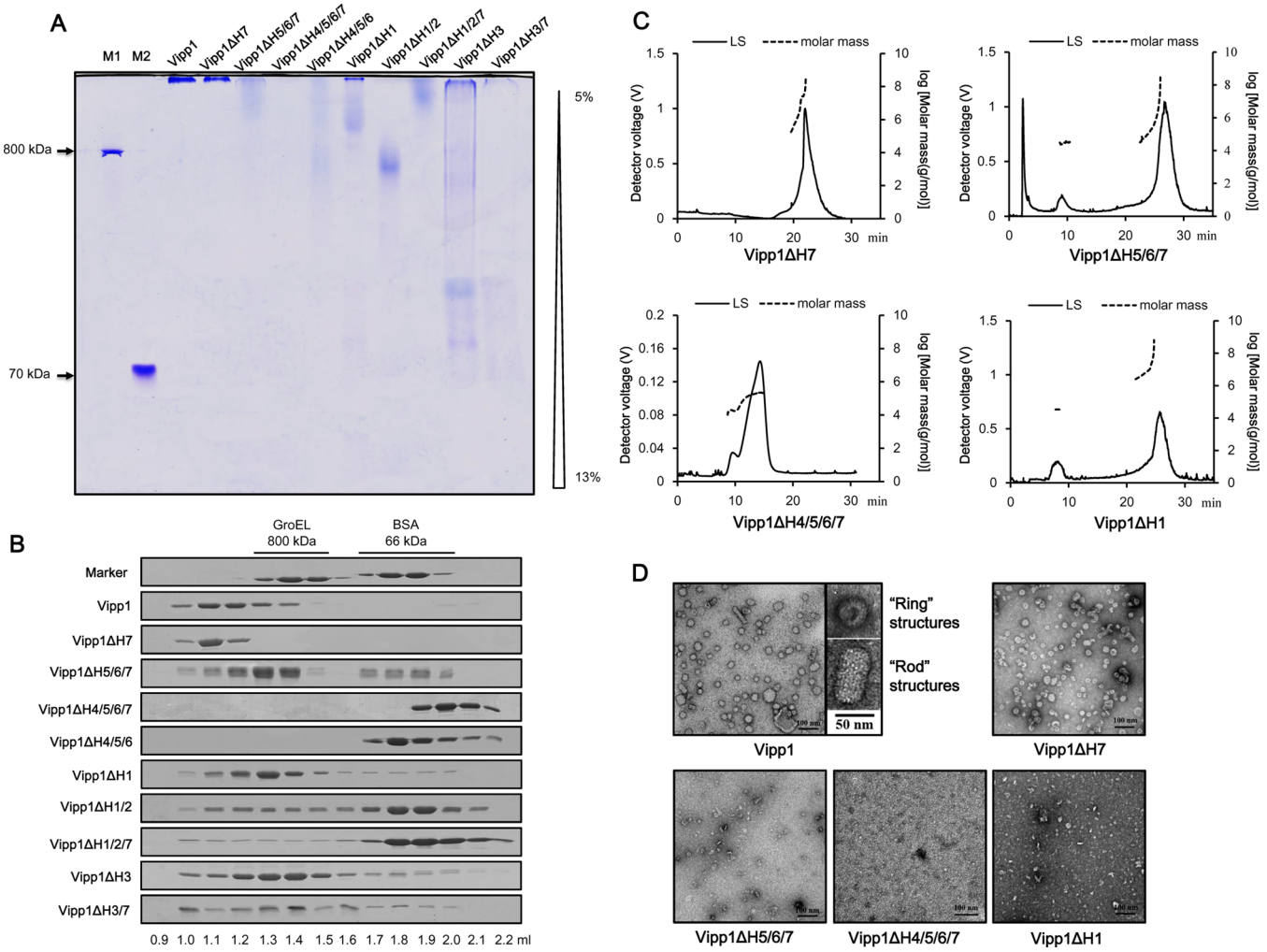

Figure 4. Oligomeric status of truncated CrVipp1 mutants. (A) Status of different truncated CrVipp1 mutants as detected by colorless 5 to 13% gradient native PAGE and staining with Coomassie brilliant blue. Ten micrograms of each truncated proteins was analyzed using the native PAGE assay. Lane M1 contained GroEL as a 800 kDa marker, and lane M2 contained GroES as a 70 kDa marker. (B) Gel filtration of CrVipp1 variants. Proteins were separated on a gel filtration column (Superose 6 PC 3.2/30, GE Healthcare) with a flow rate of 60 μL/min, and the collected fractions (100 μL each) from 0.9 to 2.2 mL were separated by 15% SDS−PAGE followed by staining with Coomassie brilliant blue. GroEL (800 kDa) and BSA (66 kDa) were loaded as controls (Marker). (C) Truncated CrVipp1 proteins were analyzed by AFFFF−MALS. LS means the signal strength of the laser detector of AFFFF shown on the left *y*-axis, and molar mass means the molecular weight of the homo-oligomer complex of truncated CrVipp1 shown on the right *y*-axis. Four truncated proteins [Vipp1ΔH1 (elution flow of 0.8 mL/min and cross-flow of 0.5 to 0 mL/min), Vipp1ΔH7 (elution flow of 0.8 mL/min and cross-flow of 0.5 to 0 mL/min), Vipp1ΔH5/6/7 (elution flow of 0.8 mL/min and cross-flow of 1 to 0 mL/min), and Vipp1ΔH4/5/6/7 (elution flow of 0.8 mL/min and cross-flow of 2 to 0 mL/min)] are shown here. (D) Transmission electron micrograph CCD images of full-length Vipp1 and truncated Vipp1 mutants. Larger magnifications of the TEM micrographs show the "ring" and "rod" structures of CrVipp1. Black bars represent a scale of 50 or 100 nm.

Interaction of CrVipp1 Variants with DnaK. Previous studies reported that Vipp1 forms both superoligomeric complexes and monomers or dimers *in vivo*, and that Vipp1 interacts with Hsp70/DnaK, which in turn is able to regulate the assembly state of Vipp1 oligomers.[22] This indicates that Hsp70/DnaK may play important roles in the structural dynamics and function of Vipp1. To determine the influence of CrVipp1 domain deletion on its interaction with DnaK, all truncated CrVipp1 proteins containing C-terminal His tags (in plasmid pET22b) and the DnaK system (in plasmid pG-KJE8) were co-expressed in *E. coli,* and pull-down experiments were performed. As shown in Figure 5A, both DnaK and truncated CrVipp1 proteins were stably expressed upon induction. With full-length Vipp1 and Vipp1ΔH7, relatively little DnaK was pulled down (Figure 5B, lanes 2, 3, and 7), indicating the interaction between DnaK and superoligomeric Vipp1 was weak, while the capacity of DnaK to bind to several truncated proteins (Figure 5B, lanes 4, 6, and 8−11) was markedly enhanced (Figure 5B). Notably, substantial DnaK was pulled down with Vipp1ΔH5/6/7 and Vipp1ΔH4/5/6, but not with Vipp1ΔH4/5/6/7 (Figure 5B, lanes 4−6), indicating DnaK interacts with these smaller oligomeric variants of Vipp1 mainly via H4 and H7 domains (Figure 5B). The capacity of DnaK to bind to CrVipp1 was normalized in Figure 5C. The capacity of DnaK to bind to certain aberrantly folded CrVipp1 mutants was enhanced up to 10-fold compared to the capacity to bind to compact superoligomeric CrVipp1. Normalization also revealed that DnaK did not bind to Vipp1ΔH1 significantly more than full-length Vipp1 (Figure 5C), probably because Vipp1ΔH1 forms large amounts of superoligomer and the DnaK system does not largely recognize it as being misfolded (Figure 4B). These results suggest that Hsp70/DnaK binds misfolded

DOI: 10.1021/acs.biochem.5b00050
Biochemistry 2015, 54, 4877−4889

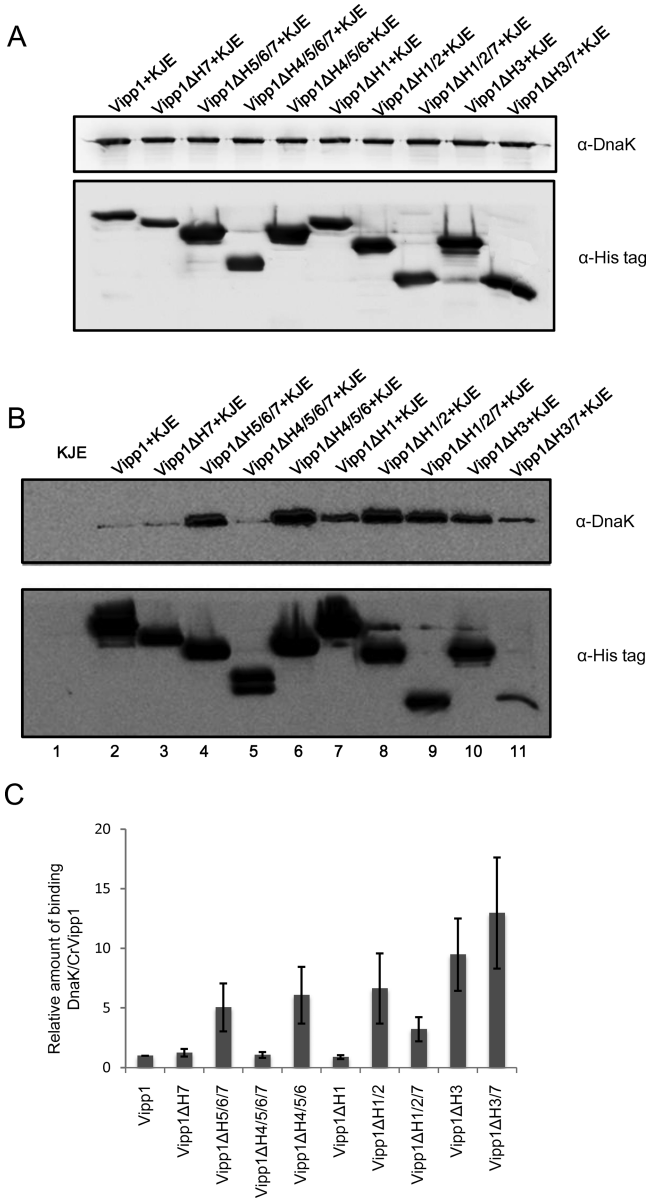

Figure 5. Secondary and tertiary structures affecting the interaction of CrVipp1 and DnaK. (A) Expression of truncated CrVipp1 proteins and DnaK in *E. coli* BL21(ED3). Both truncated CrVipp1 and DnaK were transformed into *E. coli* BL21(ED3) and induced by 0.5 mM IPTG and 0.2% L-arabinose. All induced proteins were separated by 15% SDS−PAGE, probed by anti-His and anti-DnaK serum, and detected by chemical fluorescence autoradiography. (B) Pull-down assay of truncated CrVipp1 mutants and DnaK. Proteins were eluted with 0.5 M imidazole in the pull-down experiment, resolved by 15% SDS−PAGE, probed by anti-His tag and anti-DnaK serum, and detected by chemical fluorescence autoradiography. (C) Ratios of bound DnaK and truncated protein averaged from six individual pull-down experiments with standard deviations. ImageJ was used to measure the signal intensity from Western blot results, and the ratio presents the signal intensity of pulled down DnaK to pulled down Vipp1.

Vipp1, likely via H4 and H7 domains exposed in noncompact structures, whereas Hsp70/DnaK no longer binds Vipp1 when H4 and H7 domains are properly incorporated into super-oligomeric complexes.

DnaK Interacts with CrVipp1 at an Early Stage in CrVipp1 Biogenesis. To investigate the interaction of DnaK and CrVipp1 during CrVipp1 synthesis or folding, pull-down experiments were performed after two proteins were induced for different periods of time. Specifically, the DnaK system was induced for 2 h while CrVipp1 was simultaneously induced for 15 min, 30 min, 45 min, 1 h, or 2 h, and pull-down experiments were performed to capture complexes from cell extracts (Figure 6A). The amounts of both CrVipp1 and DnaK were tightly controlled by the induction time, and the amount of induced DnaK was much greater than that pulled down with CrVipp1 (Figure 6A, lanes 6−10). Increasing the amount of CrVipp1 in cells caused the amount of pulled-down DnaK to increase slightly (Figure 6A, lanes 1−5), indicating that no matter how much CrVipp1 was expressed in the cells, the amount of DnaK bound to CrVipp1 was constant. We further quantified the relative amount of pulled-down DnaK to CrVipp1 by measuring the signal intensity on the Western blot using ImageJ, and the quantification revealed that the ratio of signal intensity of pulled-down DnaK to CrVipp1 was negative relative to the amount of CrVipp1 (Figure 6B). In another experiment, CrVipp1 was induced for 2 h while DnaK was induced for 15 min, 30 min, 45 min, 1 h, or 2 h, the amounts of both CrVipp1 and DnaK were also tightly controlled by the induction time, and the amount of induced DnaK was much greater than that pulled down with CrVipp1 (Figure 6C, lanes 6−10). Increasing the amount of DnaK in cells caused the amount of pulled-down DnaK to increase synchronously (Figure 6A, lanes 1−5), and quantification revealed that the ratio of bound DnaK to CrVipp1 positively correlated with the amount of DnaK (Figure 6D), suggesting that the concentration of DnaK influences its interaction with Vipp1. Taken together, our results suggest that DnaK may interact with CrVipp1 at an early stage of CrVipp1 biosynthesis, perhaps at early steps in the folding pathway.

DISCUSSION

PspA from *E. coli* is homologous with Vipp1 at the sequence level. Vipp1 and PspA are also highly similar in protein secondary structure and therefore likely possess similar function(s). However, a distinguishing feature of Vipp1 is that it has an elongated C-terminus containing an additional α-helix (H7), a feature absent in PspA. This structure may be responsible for the functional divergence of Vipp1 in higher plants from PspA, evident because PspA cannot completely compensate for the *vipp1* deletion in *Synechocystis*.[3] The structure and function of PspA have been described well.[21] It was reported that PspA contains four α-helices (H1−H4) in contrast to the six α-helices in Vipp1 (H1−H6); the PspA H2 domain or H3 domain alone is able to form hexamers, and the H4 domain helps PspA form a 36mer ring structure.[12] There was another model proposing that PspA contains five α-helices, which is similar to the CrVipp1 secondary structure described in this work, except that a single PspA α-helix (H5) was separated into two α-helices in CrVipp1, H5 and H6, plus an additional C-terminal extension, H7.[20] In contrast to that of PspA, the tertiary structure of Vipp1 is much more complex. In addition to forming ring-shaped oligomers, Vipp1 also forms barrel-like or rod-like structures from cyanobacteria to higher plants, *in vitro*.[18,19,22] Even though it is well-known that there are at least two Vipp1 conformational states (monomer/dimer and large superoligomeric complexes) *in vivo* in *Chlamydomonas* and *Arabidopsis*, there is no evidence of the exact functionality of these two states.[24,25] Little information was obtained from analysis of the protein domains affecting the

DOI: 10.1021/acs.biochem.5b00050
Biochemistry 2015, 54, 4877−4889

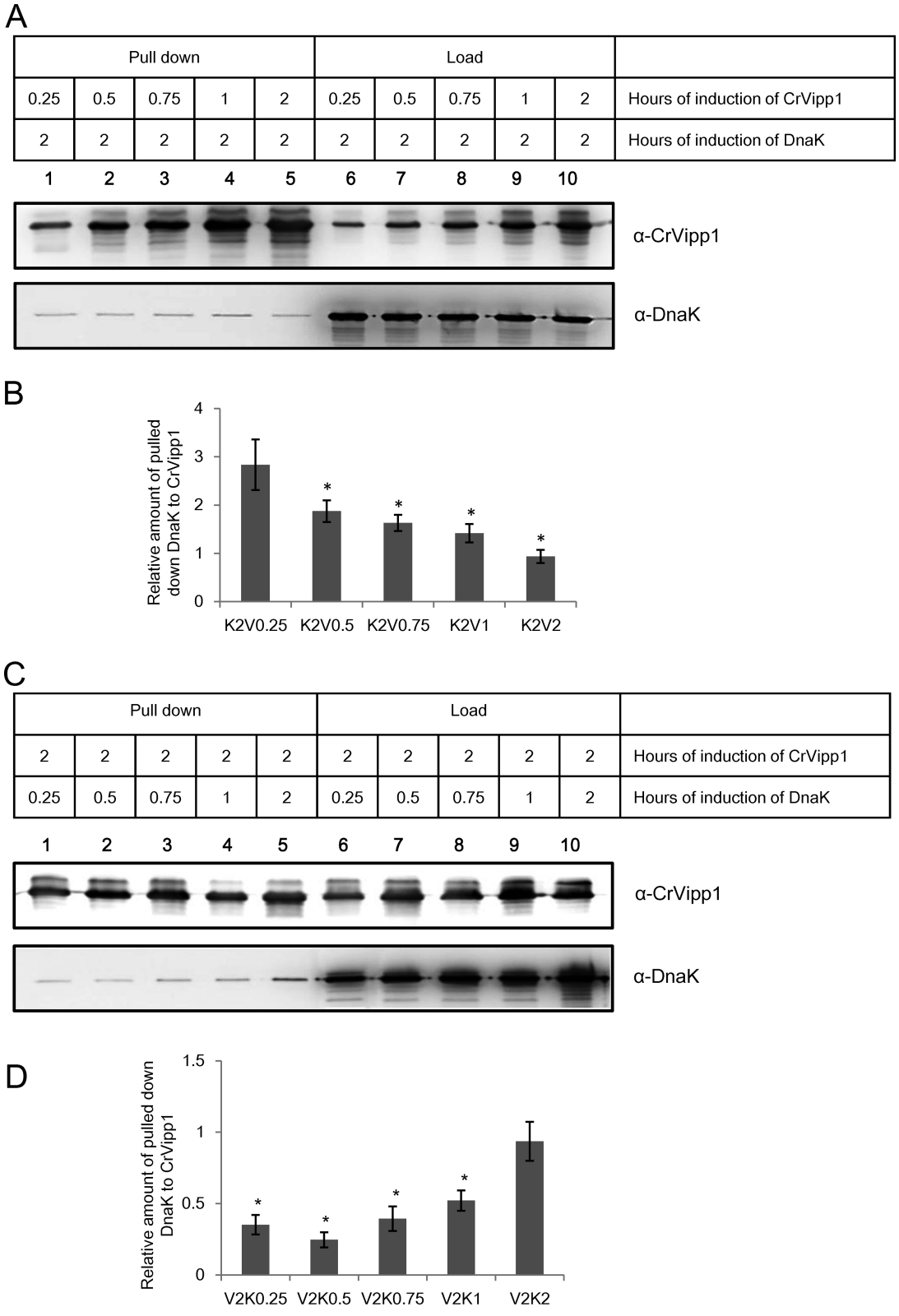

Figure 6. Kinetic analysis of the interaction between CrVipp1 and DnaK. (A) Binding efficiency of DnaK and CrVipp1 *in vivo*. CrVipp1 was induced for 2 h, and DnaK was induced for 15 min, 30 min, 45 min, 1 h, and 2 h in *E. coli* cells (as shown in the table). Pull-down analysis was conducted to capture CrVipp1−DnaK complexes. Proteins from the pull-down experiment were resolved by 15% SDS−PAGE, probed by anti-His tag and anti-DnaK serum, and detected by chemical fluorescence autoradiography. Load (lanes 6−10), components loaded into the pull-down assay. Pull down (lanes 1−5), components after the pull-down assay. (B) Ratio of pulled-down DnaK to CrVipp1 averaged over three individual pull-down experiments with standard deviations (*$p < 0.05$). V2 means CrVipp1 induced for 2 h, and K0.25, K0.5, K0.75, K1, and K2 mean DnaK induced for 15 min, 30 min, 45 min, 1 h, and 2 h, respectively. ImageJ was used to measure the signal intensity from Western blot results, and the ratio presents the signal intensity of pulled-down DnaK to Vipp1. (C) Binding efficiency of DnaK and CrVipp1 *in vivo*. DnaK was induced for 2 h, and CrVipp1 was induced for 15 min, 30 min, 45 min, 1 h, and 2 h in *E. coli* cells (as shown in the table). Pull-down analysis were conducted to capture CrVipp1−

DOI: 10.1021/acs.biochem.5b00050
Biochemistry 2015, 54, 4877−4889

Figure 6. continued

DnaK complexes. Proteins from the pull-down experiment were resolved by 15% SDS−PAGE, probed by anti-His tag and anti-DnaK serum, and detected by chemical fluorescence autoradiography. Load (lanes 6−10), components loaded into the pull-down assay. Pull down (lanes 1−5), components captured after the pull-down assay. (D) Ratio of pulled-down DnaK to CrVipp1 averaged from three individual pull-down experiments with standard deviations (*$p < 0.05$). K2 means DnaK induced for 2 h, and V0.25, V0.5, V0.75, V1, and V2 mean CrVipp1 induced for 15 min, 30 min, 45 min, 1 h, and 2 h, respectively. ImageJ was used to measure the signal intensity from Western blot results, and the ratio presents the signal intensity of pulled-down DnaK to Vipp1.

formation of different types of oligomeric complexes. It was proven that the C-terminal α-helix (H7) of AtVipp1 is dispensable in the formation of large homo-oligomers, in good agreement with our results in *Chlamydomonas*.[18,23] Furthermore, it was shown that only the first α-helix (H1) of AtVipp1 was essential for forming the superoligomer, while other helical domains had little or no effect in this process.[23]

Here, we describe systematic structural analyses of Vipp1 from *Chlamydomonas*. For this purpose, a series of deletions of individual helical domains of CrVipp1 were designed in this work. To verify truncated proteins are stable and properly folded in our system, a centrifugation assay was initially used. After centrifugation at 200000*g*, very high-molecular weight assemblies actually remained completely in the supernatant (data not shown). Furthermore, CD spectra showed all truncated proteins are nearly α-helical in structure as expected, and Vipp1, Vipp1ΔH7, Vipp1ΔH5/6/7, and Vipp1ΔH4/5/6/7 form coiled-coil structures. Finally, transmission electron microscopy was also used to check the status of all truncated proteins. It was visually verified that CrVipp1 properly folds and forms ring-like or rod-like structures with various diameters, while other truncated CrVipp1 proteins form smaller ring/rod-like structures (Figure 4D). Because all three of these assays indicated that truncated CrVipp1 proteins had ordered structure not compromised by aggregation, these truncated proteins were then further analyzed for domain-specific roles in superoligomer formation and Hsp70/DnaK interaction. Subsequent experiments indicated that the α-helical domains (H1−H6) of Vipp1 in *Chlamydomonas* have different roles in forming superoligomers. Deletion of individual helical domains or a combination of helical domains led to the accumulation of CrVipp1 in smaller oligomeric complexes that were less stable in the presence of protease. H2 and H3 might form a stable coiled-coil structure in these mutant oligomers, with H1 and H4−H6 probably functioning downstream to promote assembly of a structural core (containing H2 and H3) into larger complexes and eventually superoligomers. Interestingly, as shown in Figure 3B, the negative peak of CD spectra shifted from 208 to 203 nm in the case of Vipp1ΔH1/2, Vipp1ΔH1/2/7, Vipp1ΔH3, and Vipp1ΔH3/7. There may be two reasons. One, these four truncated proteins lacking H2 or H3 domains may not be able to form coiled-coil structures, as indicated by previous reports.[31] Second, these four truncated proteins might contain more β-sheet/turn structures after helical deletion. Taken together, our work in *Chlamydomonas* indicates that α-helices H1−H6 of CrVipp1 are indeed important for superoligomer formation. In this regard, the mechanism of the structural formation of *Chlamydomonas* Vipp1 is more similar to that of *E. coli* PspA than that of *Arabidopsis* Vipp1.

Aseeva et al. suggested that Vipp1 functionality was closely linked to the oligomeric state of Vipp1.[18] In addition, Vipp1 was able to interact with the Hsp70/DnaK system, which catalyzed the assembly of Vipp1 oligomers, suggesting that the Hsp70/DnaK system might play important roles in the structural dynamics and functionality of Vipp1.[12,22] Our results showed that the binding capacity of DnaK for Vipp1, Vipp1ΔH1, Vipp1ΔH7, and Vipp1ΔH4/5/6/7 was much lower than for other truncated proteins. Vipp1, Vipp1ΔH1, and Vipp1ΔH7 did not bind efficiently to DnaK probably because they formed high levels of superoligomers, a native state that may be weakly recognized by the DnaK system. Vipp1ΔH4/5/6/7, on the other hand, did not efficiently bind to DnaK apparently because it contains deletions in H4 and H7, putative DnaK recognition sites in misfolded proteins. In contrast, Vipp1ΔH5/6/7, Vipp1ΔH4/5/6, Vipp1ΔH1/2, Vipp1ΔH3, and Vipp1ΔH3/7 mutants, which did not form superoligomers efficiently, bound strongly to DnaK. Our results therefore suggest that not only the α-helical domains but also the oligomeric state of CrVipp1 (Vipp1, Vipp1ΔH7, and Vipp1ΔH1) affected its capacity to bind to DnaK. We also found that DnaK prefers to bind CrVipp1 shortly after induction when CrVipp1 likely has not achieved its oligomeric state. In addition, the interaction between DnaK and CrVipp1 correlated with the concentration of DnaK and was negatively related to the concentration of CrVipp1. This indicated that no matter how much CrVipp1 was expressed in the cell, the concentration of CrVipp1−DnaK complexes did not change. Taken together, our results suggest that DnaK binds preferentially to CrVipp1 or perhaps smaller species of CrVipp1 (dimers, monomers, etc.) that form early in the folding pathway of CrVipp1. This resonates with previous conclusions that the Hsp70/DnaK system might assist in the assembly of CrVipp1 superoligomers by binding non-native or smaller species.[22]

In this study, a series of truncated CrVipp1 proteins lacking different α-helical domains were used to investigate the structural and functional properties of CrVipp1. Structural analyses of CrVipp1 revealed more structural similarity to PspA than to AtVipp1. Truncated proteins derived from CrVipp1 were soluble and stable and maintained high levels of α-helical structure in our experimental system. Each of the α-helical domains of CrVipp1 was found to play unique and important roles in the formation of CrVipp1 higher-order tertiary structure. The interaction between CrVipp1 and DnaK was also investigated in the *E. coli* system. Both helical domains H4 and H7 as well as the tertiary structure of CrVipp1 affected interaction with DnaK. Further experiments suggested that DnaK may interact with CrVipp1 to help CrVipp1 assemble into higher-order oligomeric complexes. These experiments were conducted in the *E. coli* system, and further experiments in the native system will be needed to confirm the observations presented here. It is worth noting that there are several conformational states of CrVipp1 known *in vivo* (dimer/monomer and superoligomers), but the *in vitro* system used here reconstitutes predominantly the formation of superoligomers of CrVipp1. It therefore remains a possibility that the DnaK/Hsp70 system and/or other unknown factors bind to misfolded/unfolded Vipp1 to also promote the formation of dimers and monomers in addition to the superoligomers

DOI: 10.1021/acs.biochem.5b00050
Biochemistry 2015, 54, 4877−4889

studied here. Our future work will focus on studying the structural dynamics and functional mechanism of CrVipp1 and the key factors required in this process *in vivo*.

■ ASSOCIATED CONTENT

Supporting Information

Primer pairs in cloning the recombined truncated CrVipp1 proteins (Table S1). The Supporting Information is available free of charge on the ACS Publications website at DOI: 10.1021/acs.biochem.5b00050.

■ AUTHOR INFORMATION

Corresponding Authors

*E-mail: feigao@genetics.ac.cn. Telephone: +86-010-64806574. Fax: +86-010-64801360.

*E-mail: cmliu@genetics.ac.cn. Telephone: +86-010-64801360. Fax: +86-010-64801360.

Funding

This work was supported by the National Natural Science Foundation of China (31300203), the State Key Laboratory of Plant Cell and Chromosome Engineering (Grant PCCE-2012-TD-01), and the Ministry of Agriculture of China (Grant 2011ZX08009-003-005).

Notes

The authors declare no competing financial interest.

■ ACKNOWLEDGMENTS

We thank Sarah Schäuffelhut for critical reading of the manuscript and Yongsheng Chen for assistance in data acquisition using TEM.

■ ABBREVIATIONS

Vipp1, vesicle-inducing protein in plastids 1; PspA, phage shock protein A; PBS, phosphate-buffered saline; AFFFF, asymmetric flow field flow fractionation; CD, circular dichroism; PMSF, phenylmethanesulfonyl fluoride; IPTG, isopropyl β-D-galactopyranoside; EDTA, 2,2′,2″,2‴-(ethane-1,2-diyldinitrilo)-tetraacetic acid; SDS−PAGE, sodium dodecyl sulfate−polyacrylamide gel electrophoresis.

■ REFERENCES

(1) Li, H.-m., Kaneko, Y., and Keegstra, K. (1994) Molecular cloning of a chloroplastic proteinassociated with both the envelope and thylakoid membranes. *Plant Mol. Biol. 25*, 619−632.

(2) Kroll, D., Meierhoff, K., Bechtold, N., Kinoshita, M., Westphal, S., Vothknecht, U. C., Soll, J., and Westhoff, P. (2001) VIPP1, a nuclear gene of Arabidopsis thaliana essential for thylakoid membrane formation. *Proc. Natl. Acad. Sci. U. S. A. 98*, 4238−4242.

(3) Westphal, S., Heins, L., Soll, J., and Vothknecht, U. C. (2001) Vipp1 deletion mutant of Synechocystis: a connection between bacterial phage shock and thylakoid biogenesis? *Proc. Natl. Acad. Sci. U. S. A. 98*, 4243−4248.

(4) Westphal, S., Soll, J., and Vothknecht, U. C. (2001) A vesicle transport system inside chloroplasts. *FEBS Lett. 506*, 257−261.

(5) Vothknecht, U. C., and Soll, J. (2005) Chloroplast membrane transport: interplay of prokaryotic and eukaryotic traits. *Gene 354*, 99−109.

(6) Benning, C., Xu, C., and Awai, K. (2006) Non-vesicular and vesicular lipid trafficking involving plastids. *Curr. Opin. Plant Biol. 9*, 241−247.

(7) Aseeva, E., Ossenbuhl, F., Sippel, C., Cho, W. K., Stein, B., Eichacker, L. A., Meurer, J., Wanner, G., Westhoff, P., Soll, J., and Vothknecht, U. C. (2007) Vipp1 is required for basic thylakoid membrane formation but not for the assembly of thylakoid protein complexes. *Plant Physiol. Biochem. 45*, 119−128.

(8) Gao, H., and Xu, X. (2009) Depletion of Vipp1 in Synechocystis sp. PCC 6803 affects photosynthetic activity before the loss of thylakoid membranes. *FEMS Microbiol. Lett. 292*, 63−70.

(9) Nordhues, A., Schottler, M. A., Unger, A. K., Geimer, S., Schonfelder, S., Schmollinger, S., Rutgers, M., Finazzi, G., Soppa, B., Sommer, F., Muhlhaus, T., Roach, T., Krieger-Liszkay, A., Lokstein, H., Crespo, J. L., and Schroda, M. (2012) Evidence for a role of VIPP1 in the structural organization of the photosynthetic apparatus in Chlamydomonas. *Plant Cell 24*, 637−659.

(10) Lo, S. M., and Theg, S. M. (2012) Role of vesicle-inducing protein in plastids 1 in cpTat transport at the thylakoid. *Plant J. 71*, 656−668.

(11) Brissette, J. L., Russel, M., Weiner, L., and Model, P. (1990) PHAGE SHOCK PROTEIN, A STRESS PROTEIN OF ESCHERICHIA-COLI. *Proc. Natl. Acad. Sci. U. S. A. 87*, 862−866.

(12) Vothknecht, U. C., Otters, S., Hennig, R., and Schneider, D. (2012) Vipp1: a very important protein in plastids?! *J. Exp. Bot. 63*, 1699−1712.

(13) Model, P., Jovanovic, G., and Dworkin, J. (1997) The Escherichia coli phage-shock-protein (psp) operon. *Mol. Microbiol. 24*, 255−261.

(14) Darwin, A. J. (2005) The phage-shock-protein response. *Mol. Microbiol. 57*, 621−628.

(15) Joly, N., Engl, C., Jovanovic, G., Huvet, M., Toni, T., Sheng, X., Stumpf, M. P., and Buck, M. (2010) Managing membrane stress: the phage shock protein (Psp) response, from molecular mechanisms to physiology. *FEMS microbiology reviews 34*, 797−827.

(16) Zhang, L., Kato, Y., Otters, S., Vothknecht, U. C., and Sakamoto, W. (2012) Essential role of VIPP1 in chloroplast envelope maintenance in Arabidopsis. *Plant Cell 24*, 3695−3707.

(17) DeLisa, M. P., Lee, P., Palmer, T., and Georgiou, G. (2004) Phage Shock Protein PspA of Escherichia coli Relieves Saturation of Protein Export via the Tat Pathway. *J. Bacteriol. 186*, 366−373.

(18) Aseeva, E., Ossenbuhl, F., Eichacker, L. A., Wanner, G., Soll, J., and Vothknecht, U. C. (2004) Complex formation of Vipp1 depends on its alpha-helical PspA-like domain. *J. Biol. Chem. 279*, 35535−35541.

(19) Fuhrmann, E., Bultema, J. B., Kahmann, U., Rupprecht, E., Boekema, E. J., and Schneider, D. (2009) The vesicle-inducing protein 1 from Synechocystis sp. PCC 6803 organizes into diverse higher-ordered ring structures. *Molecular biology of the cell 20*, 4620−4628.

(20) Bultema, J. B., Fuhrmann, E., Boekema, E. J., and Schneider, D. (2010) Vipp1 and PspA: Related but not twins. *Commun. Integr. Biol. 3*, 162−165.

(21) Hankamer, B. D., Elderkin, S. L., Buck, M., and Nield, J. (2004) Organization of the AAA(+) adaptor protein PspA is an oligomeric ring. *J. Biol. Chem. 279*, 8862−8866.

(22) Liu, C., Willmund, F., Golecki, J. R., Cacace, S., Hess, B., Markert, C., and Schroda, M. (2007) The chloroplast HSP70B-CDJ2-CGE1 chaperones catalyse assembly and disassembly of VIPP1 oligomers in Chlamydomonas. *Plant J. 50*, 265−277.

(23) Otters, S., Braun, P., Hubner, J., Wanner, G., Vothknecht, U. C., and Chigri, F. (2013) The first alpha-helical domain of the vesicle-inducing protein in plastids 1 promotes oligomerization and lipid binding. *Planta 237*, 529−540.

(24) Liu, C., Willmund, F., Whitelegge, J. P., Hawat, S., Knapp, B., Lodha, M., and Schroda, M. (2005) J-domain protein CDJ2 and HSP70B are a plastidic chaperone pair that interacts with vesicle-inducing protein in plastids 1. *Molecular biology of the cell 16*, 1165−1177.

(25) Feng, J., Fan, P., Jiang, P., Lv, S., Chen, X., and Li, Y. (2014) Chloroplast-targeted Hsp90 plays essential roles in plastid development and embryogenesis in Arabidopsis possibly linking with VIPP1. *Physiol. Plant. 150*, 292−307.

(26) Asamizu, E., Nakamura, Y., Miura, K., Fukuzawa, H., Fujiwara, S., Hirono, M., Iwamoto, K., Matsuda, Y., Minagawa, J., and Shimogawara, K. (2004) Establishment of publicly available cDNA

DOI: 10.1021/acs.biochem.5b00050
Biochemistry 2015, 54, 4877−4889

material and information resource of Chlamydomonas reinhardtii (Chlorophyta) to facilitate gene function analysis. *Phycologia 43*, 722−726.
(27) Laemmli, U. K. (1970) Cleavage of structural proteins during the assembly of the head of bacteriophage T4. *Nature 227*, 680−685.
(28) Khater, L., Alegria, M. C., Borin, P. F., Santos, T. M., Docena, C., Tasic, L., Farah, C. S., and Ramos, C. H. (2007) Identification of the flagellar chaperone FlgN in the phytopathogen Xanthomonas axonopodis pathovar citri by its interaction with hook-associated FlgK. *Arch. Microbiol. 188*, 243−250.
(29) Qiu, Y., Niu, H., Huang, W., He, Y., and Wu, X.-H. (2011) Properties and secondary structure of tannase from Penicillium herquei. *Biotechnol. Bioprocess Eng. 16*, 858−866.
(30) Monera, O., Zhou, N., Kay, C., and Hodges, R. (1993) Comparison of antiparallel and parallel two-stranded alpha-helical coiled-coils. Design, synthesis, and characterization. *J. Biol. Chem. 268*, 19218−19227.
(31) Lau, S. Y., Taneja, A. K., and Hodges, R. S. (1984) Synthesis of a model protein of defined secondary and quaternary structure. Effect of chain length on the stabilization and formation of two-stranded alpha-helical coiled-coils. *J. Biol. Chem. 259*, 13253−13261.

DOI: 10.1021/acs.biochem.5b00050
Biochemistry 2015, 54, 4877−4889